

# Optical Properties of Ultrathin Poly(3,4-ethylenedioxythiophene) Films at Several Doping Levels Studied by In Situ Electrochemical Surface Plasmon Resonance Spectroscopy

Akira Baba,<sup>†,‡</sup> Jörn Lübben,<sup>‡</sup> Kaoru Tamada,<sup>†,§</sup> and Wolfgang Knoll<sup>\*,†,‡</sup>

Departments of Chemistry and of Materials Science, National University of Singapore, 10 Science Drive 4, Lower Kent Ridge Road, Singapore, 117543, Singapore, Max-Planck-Institute for Polymer Research, Ackermannweg 10, 55128 Mainz, Germany, and National Institute of Advanced Industrial Science and Technology (AIST), Tsukuba Center 5, 1-1-1 Higashi, Tsukuba, Ibaraki 305-8565, Japan

Received May 16, 2003. In Final Form: August 5, 2003

In this paper, we report on in situ optical/electrochemical investigations using a combination of surface plasmon resonance spectroscopy and electrochemistry in order to determine the complex dielectric constants of poly(3,4-ethylenedioxythiophene) (PEDOT) thin films. The PEDOT films were deposited by in situ electropolymerization. The film thickness was monitored by a quartz crystal microbalance. In the electrochemical surface plasmon resonance (EC-SPR) measurements, three wavelengths corresponding to interband and intraband electronic transition regions were used in order to investigate electrochromic properties. The optical conductivity was also determined by EC-SPR measurement with a near-infrared laser wavelength which corresponds to the region outside the anomalous dispersion.

## Introduction

Poly(3,4-ethylenedioxythiophene) (PEDOT) is a very well studied conjugated polymer, owing to many attractive properties such as its electrical conductivity ( $\sim 550$  S/cm), a low band gap (1.5–1.7 eV), transparency in the conducting state, a high contrast in the visible region upon electrochromic switching, and so forth.<sup>1,2</sup> When its de-doped state is switched to the doped state, a significant color change occurs from dark blue to transparent sky blue. Because of its interesting electronic properties, applications as transparent electrodes,<sup>3,4</sup> hole-injecting layers for organic light-emitting diodes,<sup>5–7</sup> sensors,<sup>8,9</sup> photodiodes,<sup>10</sup> and electrochromic windows<sup>11–13</sup> have been proposed. However, a deeper understanding of the optoelectronic properties of ultrathin PEDOT films is necessary for further device applications. Electropolymerized films have been studied extensively in order to understand the intrinsic properties of the polymer. Various techniques,

such as in situ UV–vis spectroscopy, Fourier transform infrared (FT-IR) spectroscopy,<sup>14</sup> atomic force microscopy (AFM), X-ray photoelectron spectroscopy (XPS),<sup>15</sup> and electrochemical quartz crystal microbalance (EQCM)<sup>16</sup> studies, have been applied to investigate the film formation, structural and volume changes, and the ion transport upon doping and de-doping. However, there is still a considerable uncertainty in the determination of the complex dielectric constants, the conductivity, and so forth at different doping levels.

Surface plasmon resonance (SPR) spectroscopy is a technique of high sensitivity for characterizing ultrathin films at the nanometer thickness scale.<sup>17</sup> The combination of surface plasmon resonance spectroscopy (SPS) with electrochemical (EC) measurements has been demonstrated to be a powerful technique for the simultaneous characterization and manipulation of electrode/electrolyte interfaces.<sup>18–20</sup> Recently, the EC-SPS technique also has been applied for the characterization of conducting polymer films.<sup>21–28</sup> This involved the in situ monitoring of the swelling/shrinking behavior and of electrochromic

<sup>†</sup> National University of Singapore.

<sup>‡</sup> Max-Planck-Institute for Polymer Research.

<sup>§</sup> National Institute of Advanced Industrial Science and Technology (AIST).

(1) Pettersson, L. A. A.; Carlsson, F.; Inganäs, O.; Arwin, H. *Thin Solid Films* **1998**, *313–314*, 356.

(2) Groenendaal, L.; Jonas, F.; Freitag, D.; Pielartzik, H.; Reynolds, J. R. *Adv. Mater.* **2000**, *12*, 481.

(3) Bayer AG, European Patent 686 662, 1995.

(4) Chang, Y.; Lee, K.; Kiebooms, R.; Aleshin, A.; Heeger, A. J. *Synth. Met.* **1999**, *105*, 203.

(5) Granstrom, M.; Berggren, M.; Inganäs, O. *Science* **1995**, *267*, 1479.

(6) Bharathan, J. M.; Yang, Y. *Appl. Phys. Lett.* **1998**, *84*, 3207.

(7) Cao, Y.; Yu, G.; Zhang, C.; Menon, R.; Heeger, A. J. *Synth. Met.* **1997**, *87*, 171.

(8) Yamato, H.; Ohwa, M.; Wernet, W. *J. Electroanal. Chem.* **1995**, *397*, 163.

(9) Babacka, J. *Anal. Chem.* **1999**, *71*, 4932.

(10) Arias, A. C.; Granstrom, M.; Petritsch, K.; Friend, R. H. *Synth. Met.* **1999**, *102*, 953.

(11) Gustafsson, J. C.; Liedberg, B.; Inganäs, O. *Solid State Ionics* **1994**, *69*, 145.

(12) Sotzing, G. A.; Reddinger, J. L.; Reynolds, J. R.; Steel, P. J. *Synth. Met.* **1997**, *84*, 199.

(13) Reynolds, J. R. *Adv. Mater.* **1996**, *8*, 808.

(14) Kvarnstrom, C.; Neugebauer, H.; Blomquist, S.; Ahonen, H. J.; Kankare, J.; Ivaska, A. *Electrochim. Acta* **1999**, *44*, 2739.

(15) Xing, K. Z.; Fahlman, M.; Chen, X. W.; Inganäs, O.; Salaneck, W. R. *Synth. Met.* **1997**, *89*, 161.

(16) Paik, W.; Yeo, I. H.; Suh, H.; Kim, Y.; Song, E. *Electrochim. Acta* **2000**, *45*, 3833.

(17) Knoll, W. *Annu. Rev. Phys. Chem.* **1998**, *49*, 569.

(18) Tadjeddine, A.; Kolb, D. M.; Kötzt, R. *Surf. Sci.* **1980**, *101*, 277.

(19) Gordon, J. G., II; Ernst, S. *Surf. Sci.* **1980**, *101*, 499.

(20) Iwasaki, Y.; Horiuchi, T.; Morita, M.; Niwa, O. *Electroanalysis* **1997**, *9*, 1239.

(21) Baba, A.; Advincula, R. C.; Knoll, W. *PMSE Prepr.* **2001**, *84*, 369.

(22) Baba, A.; Advincula, R. C.; Knoll, W. *J. Phys. Chem. B* **2002**, *106*, 1581.

(23) Baba, A.; Park, M.-K.; Advincula, R. C.; Knoll, W. *Langmuir* **2002**, *18*, 4648.

(24) Xia, C.; Advincula, R.; Baba, A.; Knoll, W. *Langmuir* **2002**, *18*, 3555.

(25) Baba, A.; Knoll, W. *Adv. Mater.* **2003**, *15*, 1015.

(26) Chegel, V.; Raitman, O.; Katz, E.; Gabai, R.; Willner, I. *Chem. Commun.* **2001**, 883.

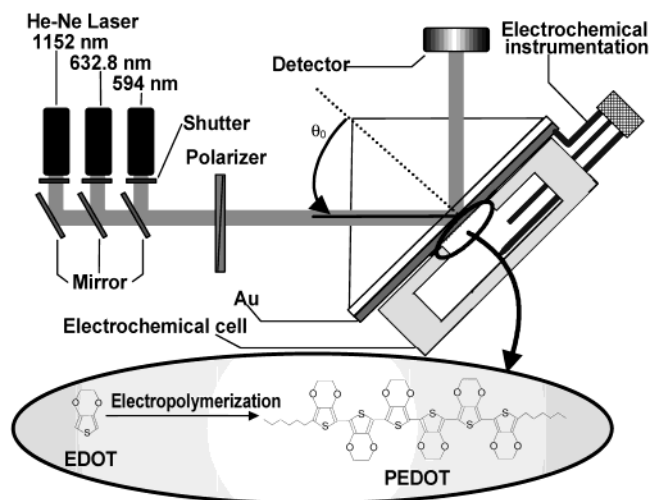


**Figure 1.** ATR setup used for the excitation of surface plasmons in the Kretschmann geometry: a thin metal film is evaporated onto the base of a glass prism and acts as a resonator driven by the photon field. Three different He–Ne laser wavelengths were used:  $\lambda = 594$  nm,  $\lambda = 632.8$  nm, and  $\lambda = 1152$  nm.

properties during the electropolymerization process or during anion doping/de-doping of the deposited polymers. This technique has also been applied for the development of biosensors via the integration of redox enzymes with the conducting polymers as a bioelectrocatalytic layer.<sup>29,30</sup> Surface plasmon enhanced light scattering (SPLS),<sup>14–16</sup> surface plasmon enhanced photoluminescence (SPPL),<sup>31</sup> and the quartz crystal microbalance (QCM) technique<sup>32,33</sup> have also been reported in combination with EC-SPS for the characterization of conducting polymer layers.

In this study, we describe the quantitative analysis of ultrathin PEDOT films at several doping levels by the in situ EC-SPS technique. The deposition process monitored by the QCM allows for the determination of the amount of charge transferred from each monomer during the electropolymerization process. Three lasers with different wavelengths covering the inter- and intraband electronic transition region were used to investigate the electrochromism of PEDOT films at several doping levels. The optical conductivity, that is, the conductivity derived from analyzing the imaginary part of the dielectric function, was measured with a laser wavelength in the region of the intraband transition energy ( $\lambda = 1152$  nm). The complex dielectric constant and optical conductivity of the conducting polymer ultrathin film at several doping levels are determined accurately by use of this in situ technique.

### Experimental Section

**Materials.** 3,4-Ethylenedioxythiophene (EDOT) and tetrabutylammonium hexafluorophosphate were purchased from Aldrich and used as received.

**Electrochemical Measurement.** Electrochemical experiments were performed in a conventional three-electrode cell with the Au/LaSFN9 glass substrate as the working electrode, a platinum wire as the counter electrode, and an Ag/Ag<sup>+</sup> non-

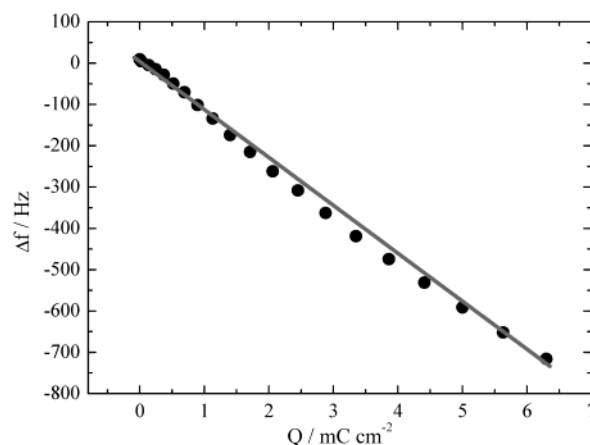


**Figure 2.** Frequency change ( $\Delta f$ ) in the QCM measurement as a function of the amount of charge,  $Q$ , transferred during the electropolymerization of EDOT at  $E = 0.9$  V (vs Ag/Ag<sup>+</sup>). The solid line is a linear fit to the experimental results (full dots).

aqueous reference electrode. A potentiostat (Princeton Applied Research 263A, EG&G) was used for the cyclic voltammetry experiments. Electropolymerization was done from 0.01 MEDOT monomer in acetonitrile solution with 0.1 M TBAPF<sub>6</sub>. Electrochemical measurements in monomer-free solution were performed in acetonitrile solution with 0.1 M TBAPF<sub>6</sub>.

**Electrochemical SPS.** Figure 1 shows the attenuated total reflection (ATR) setup used for the excitation of surface plasmons in the Kretschmann configuration combined with an electrochemical cell. A triangle LaSFN9 prism was used.<sup>17</sup> The Au/glass substrates were clamped against the Teflon cell with an O-ring providing a liquid-tight seal. The Teflon cell was then mounted to the two-axis goniometer for investigations by SPR. Surface plasmons are excited at the metal–dielectric interface, upon total internal reflection of a polarized laser light beam. Three wavelengths, that is,  $\lambda = 632.8$  nm,  $\lambda = 594$  nm, and  $\lambda = 1152$  nm, of a He–Ne laser were used in all measurements. The optical/electrochemical processes on the gold were detected by monitoring the reflectivity as a function of the incident angle  $\theta_0$ .

**EQCM Measurement.** Commercial 5 MHz AT-cut quartz crystals with Au electrodes in a crystal holder (Maxtek Inc., USA) were used. The front electrode of the crystal was used as the working electrode, with the back electrode being grounded. Both electrodes were connected at the backside to an impedance analyzer. On both sides of the crystal, O-rings were used to prevent leakage. Details concerning this setup can be found elsewhere.<sup>34</sup> The crystals were cleaned by sonication in acetone, Hellmanex, and Milli-Q water following plasma cleaning before the measurements with an impedance analyzer (HP 4396A, 100 kHz–1.8 GHz, Hewlett-Packard). To separate the radio frequency (rf) voltage (network analyzer) and the direct current (dc) voltage (potentiostat), a combination of a capacitor and an inductance was used as described elsewhere.<sup>35</sup>

**Optoelectrochemical Spectroscopy.** Optoelectrochemical spectroscopy was carried out on a UV–vis–near-infrared (NIR) spectrometer (Perkin-Elmer, Lambda 9). In the optoelectrochemical measurements, an indium–tin oxide (ITO) substrate was used as the working electrode instead of the Au thin film used in the SPR and QCM measurements. Film thicknesses were measured by a Surface Profiler (Tencor P10, KLA-Tencor Corp.).

### Results and Discussion

**Electropolymerization of PEDOT.** In the QCM measurements, the quartz crystal changes its oscillation frequency as additional mass is deposited onto its electrode-coated surface. The relationship between the frequency change and the deposited mass can be rather complex for media on thin films.<sup>36</sup> For sufficiently rigid films, however, the well-known Sauerbrey equation<sup>37</sup> can

(27) Raitman, O.; Katz, E.; Willner, I.; Chegel, V.; Popova, G. *Angew. Chem., Int. Ed.* **2001**, *40*, 3649.

(28) Kang, X.; Jin, Y.; Chen, G.; Dong, S. *Langmuir* **2002**, *18*, 1713.

(29) Raitman, O. A.; Katz, E.; Bückmann, A. F.; Willner, I. *J. Am. Chem. Soc.* **2002**, *124*, 6487.

(30) Tian, S.; Baba, A.; Liu, J.; Wang, Z.; Knoll, W.; Park, M.-K.; Advincula, R. *Adv. Funct. Mater.* **2003**, *13*, 473.

(31) Baba, A.; Knoll, W. *J. Phys. Chem. B* **2003**, *107*, 7733.

(32) Bailey, L. E.; Kambhampati, D.; Kanazawa, K. K.; Knoll, W.; Frank, C. W. *Langmuir* **2002**, *18*, 479.

(33) Bund, A.; Baba, A.; Berg, S.; Johannsmann, D.; Lübben, J.; Wang, Z.; Knoll, W. *J. Phys. Chem. B* **2003**, *107*, 6743.

(34) Johannsmann, D. *Macromol. Chem. Phys.* **1999**, *200*, 501.

(35) Bund, A.; Schwitzgebel, G. *Electrochim. Acta* **2000**, *45*, 3703.

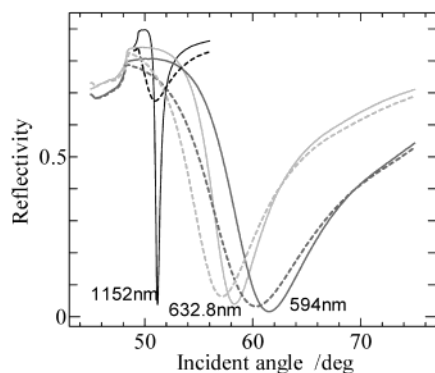


**Figure 3.** Angular SPS scans measured at three different wavelengths, as indicated (solid curve, before electropolymerization; dotted curve, after electropolymerization).

be applied with the frequency shift  $\Delta f$  (Hz) being a function of several known parameters of the QCM setup. The electrochemical polymerization of EDOT on the gold surface was initiated by applying a constant potential of  $E = 0.9$  V. The frequency change was monitored in the QCM setup as a function of the amount of charge transferred from the EDOT monomer to the electrode during electropolymerization as shown in Figure 2. The observed frequency decrease with the (transferred) charge increase indicates that the electropolymerized PEDOT film was deposited on the gold working electrode. As the change of the imaginary part of the frequency, which directly corresponds to the dissipation, in the deposited thin film was found to be only 82.0 Hz in our experiment, the Sauerbrey equation could be applied in order to relate the frequency shifts to the mass change.<sup>38</sup> As shown in Figure 2, the frequency change was almost linearly related to the amount of (transferred) charge, with  $\Delta f = 716$  Hz corresponding to about  $\Delta m = 12.7 \mu\text{g}$  and about  $\Delta d = 85.0$  nm in thickness assuming a polymer density of  $\rho = 1.5 \text{ g cm}^{-3}$ .<sup>39</sup> With this calibration, one can calculate the complex dielectric constants of the films from SPR measurements by taking into consideration the amount of mass thickness measured simultaneously with the QCM.

In EQCM measurements, the areal mass density  $m_f$  is related to the passed charge density  $Q$ .<sup>33,35</sup> In the case of electropolymerized polymers, the theoretical value of the current efficiency,  $m_f/Q$ , is calculated according to

$$\frac{m_f}{Q} = \frac{(M_M - 2M_H) + x_A M_A + x_S M_S + x_N M_N}{(2 + x_A)F} \quad (1)$$

where  $M_M$ ,  $M_A$ ,  $M_H$ ,  $M_S$ , and  $M_N$  are the molar masses of the monomer, the incorporated anion, hydrogen, the solvent, and the neutral salt, respectively;  $x_A$ ,  $x_S$ , and  $x_N$  are the molar equivalents of the doping anion, the solvent, and the neutral salt per monomer; and  $F$  is the Faraday constant ( $96485 \text{ C mol}^{-1}$ ).

The values for  $x_S M_S + x_N M_N$  of three different films prepared under similar experimental conditions are found to be 181–262 assuming  $x_A = 0.3$ , that is, 2.3 electrons per 1 monomer. This value is quite large compared to values reported for polymer layers electropolymerized in aqueous solution.<sup>35</sup> This result indicates that the PEDOT

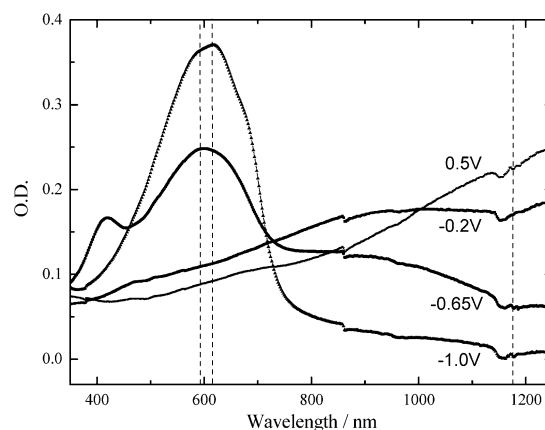


**Figure 4.** UV-vis-NIR spectra of a PEDOT film on ITO glass at different potentials applied (as indicated). The dashed lines correspond to the wavelengths used in the SPS measurements.

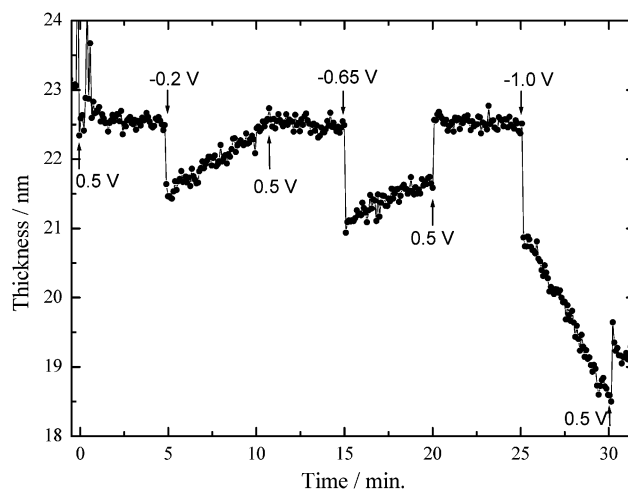


**Figure 5.** Thickness measured by the QCM of a PEDOT film at different potentials applied, as indicated.

film electropolymerized in acetonitrile contains a number of solvent and neutral salt molecules. Since one neutral salt molecule is too large to be incorporated together with one EDOT monomer, it is expected from the calculated value that one EDOT monomer is accompanied by 4–5 acetonitrile molecules.

Figure 3 shows SPR data for gold in EDOT solution (solvent, acetonitrile (ACN)) measured at three different wavelengths at open circuit potentials before and after electropolymerization. The solid curves correspond to the data before polymerization (i.e., bare gold in EDOT solution), while the dashed curves correspond to that after polymerization (i.e., a thin PEDOT film is deposited on gold in the EDOT solution). The electropolymerization was carried out at  $E = 0.9$  V for 30 s. The complex dielectric constants of the gold film  $\epsilon'_{\text{Au}} + i\epsilon''_{\text{Au}}$  were determined at each wavelength to be  $-9.8 + i1.5$  (594 nm),  $-12.7 + i1.4$  (632.8 nm), and  $-64.2 + i3.5$  (1152 nm) by fitting the angular scan curves with Fresnel's equation. The dielectric constants of the EDOT solution in ACN were also determined to be  $1.816 + i0$  (594 nm),  $1.813 + i0$  (632.8 nm), and  $1.795 + i0$  (1152 nm), respectively, by fitting the critical angle of total internal reflection. Note that the critical angle of the reflectivity curve depends only on the dielectric constant of the prism and of the monomer solution. As shown in this figure, the whole SPR curves shift toward lower angles by the PEDOT film deposition for all measurements, which suggests that the real part of the dielectric constant ( $\epsilon'$ ) of the deposited PEDOT film

(36) Reed, C.; Kanazawa, K. K.; Kaufman, J. *J. Appl. Phys.* **1990**, *68*, 1993.

(37) Sauerbrey, G. *Z. Phys.* **1959**, *155*, 206.

(38) Baba, A.; Tian, S.; Stefani, F.; Xia, C.; Wang, Z.; Advincula, R. C.; Johannsmann, J.; Knoll, W. *J. Electroanal. Chem.*, in press.

(39) Niu, L.; Kvamström, C.; Frberg, K.; Ivaska, A. *Synth. Met.* **2001**, *122*, 425.



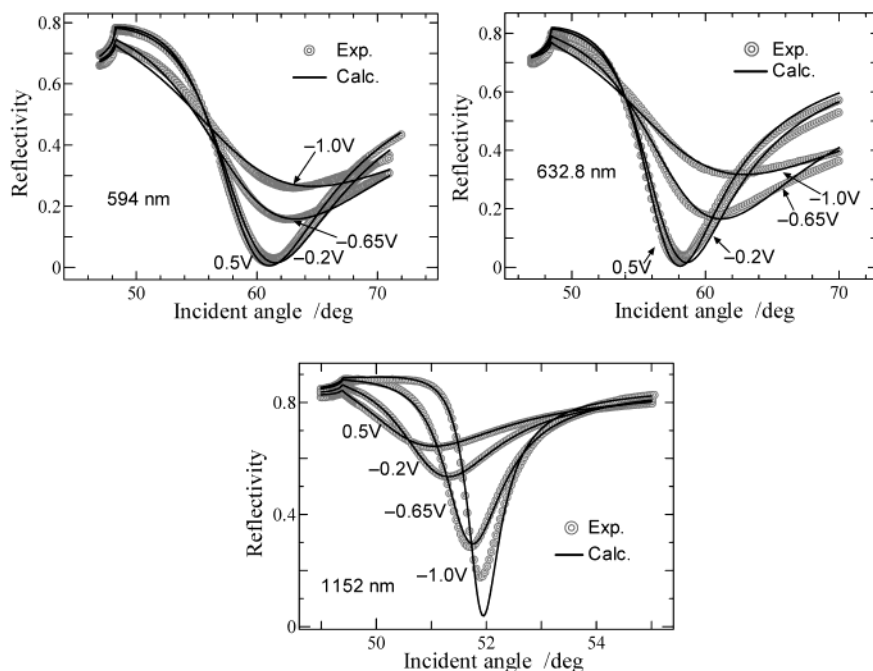


**Figure 6.** Experimental SPS reflectivity curves at different applied potentials as indicated, measured at  $\lambda = 594$  nm,  $\lambda = 632.8$  nm, and  $\lambda = 1152$  nm. The solid lines are the Fresnel simulations.

is lower than that of the EDOT solution at each wavelength. The quantitative evaluation will be discussed later.

At  $\lambda = 1152$  nm, a strongly broadened SPR curve was observed. In the SPR measurements, broadening of reflectivity curves is generally caused either by absorption at the used wavelength or by the roughness of the deposited film. In the doped state, a PEDOT film has an absorption band in the near-infrared region but has little absorption in the visible. Since the broadening of the SPR curve was observed only at  $\lambda = 1152$  nm but not at  $\lambda = 594$  nm and not at  $\lambda = 632.8$  nm, we conclude that the broadening of the SPR curve at 1152 nm originates from the strong absorption of light at this wavelength rather than from roughness.

**Electrochromic Properties of PEDOT Films.** *Optoelectrochemistry.* Transmission UV-vis-NIR spectra were taken at various applied constant potentials in order to study the electrochromic properties of PEDOT. A thin film was electropolymerized for 90 s at  $E = 0.9$  V (vs Ag/Ag<sup>+</sup>) on an ITO electrode from 0.01 M EDOT solution containing 0.1 M tetrabutylammonium hexafluorophosphate. The film thickness was estimated to be ca.  $\sim 200$  nm by surface profilometry. UV-vis-NIR measurements of the PEDOT film were taken in 0.1 M tetrabutylammonium hexafluorophosphate electrolyte solution (EDOT free) of different potentials as shown in Figure 4. As the applied potential decreased, the absorption in the visible region due to the  $\pi-\pi^*$  (interband) transition increased. In the neutral state (the state by which anion is almost de-doped from a film), the electronic band gap ( $E_g$ ) was determined to be ca. 1.7 eV ( $\lambda = 730$  nm) from the onset of the interband transition. The average transition energy of the interband transition was determined from  $\lambda_{\max}$  to be 2.04 eV ( $\lambda = 610$  nm). The absorbance in the NIR region due to the intraband transition decreased with decreasing potential. The PEDOT film became neutral at  $-1.0$  V, in good agreement with the previous reports for PEDOT films.<sup>40,41</sup> When the applied potential increases, electrons

are transferred from the PEDOT film to the electrode, so that the polaronic/bipolaronic band appeared (at this time, anion is doped into the PEDOT film in order to compensate the charge balance). This was seen by a decrease of  $\pi-\pi^*$  absorption and by an increase of the absorbance in the intraband region.

**Electrochemical QCM.** Figure 5 shows a real-time response measurement of the swelling behavior of the film monitored by EQCM, with the frequency shift being converted to thickness by the Sauerbrey equation with a density  $\rho = 1.5$  g cm<sup>-3</sup>.<sup>42</sup> The potential was switched every 5 min between the doped and the de-doped state, with a sequence of potentials of  $0.5 \rightarrow -0.2 \rightarrow 0.5 \rightarrow -0.65 \rightarrow 0.5 \rightarrow -1.0$ . When the potential was switched from 0.5 to  $-0.2$  V, the film initially shrunk and then swelled gradually. A change in volume during the doping and de-doping processes for conducting polymer films has also been reported by the other group.<sup>43-45</sup> When the potential was switched from  $-0.2$  to 0.5 V, the thickness remained constant. If the de-doping potential was switched from 0.5 to  $-0.65$  V, the film initially shrunk more than at  $-0.2$  V, and then the gradual swelling was smaller than at  $-0.2$  V. This shows that the de-doping process at  $-0.2$  and  $-0.65$  V has two regions. The initial shrinking can be caused by expelling of anions with solvent from the film. The following swelling might be caused by reinsertion of solvent due to structural reorganization of the polymer chains. Similar properties have been reported to occur during doping at around this potential.<sup>11,46</sup> When switched to  $-1.0$  V, the PEDOT film kept decreasing due to the de-doping of anion. In the simulations of the SPR experiments, the thickness value at  $\Delta t = 2.5$  min after a potential step is used because the SPR curves in our

(42) Sauerbrey, G. *Z. Phys.* **1959**, *155*, 206.

(43) Yoshino, K.; Nakao, K.; Morita, S.; Onoda, M. *Jpn. J. Appl. Phys.* **1989**, *28*, L2027.

(44) Murthy, N. S.; Shacklette, L. W.; Baughmann, R. H. *J. Chem. Phys.* **1987**, *87*, 2346.

(45) Winokur, M.; Walmsley, P.; Smith, J.; Heeger, A. J. *Macromolecules* **1991**, *24*, 3812.

(46) Chen, X.; Xing, K.-Z.; Ingañäs, O. *Chem. Mater.* **1996**, *8*, 2439.

(40) Kumar, A.; Welsh, D. M.; Morvant, M. C.; Piroux, F.; Abboud, K. A.; Reynolds, J. R. *Chem. Mater.* **1998**, *10*, 896.

(41) Sozting, G. A.; Reynolds, J. R. *Adv. Mater.* **1997**, *9*, 795.

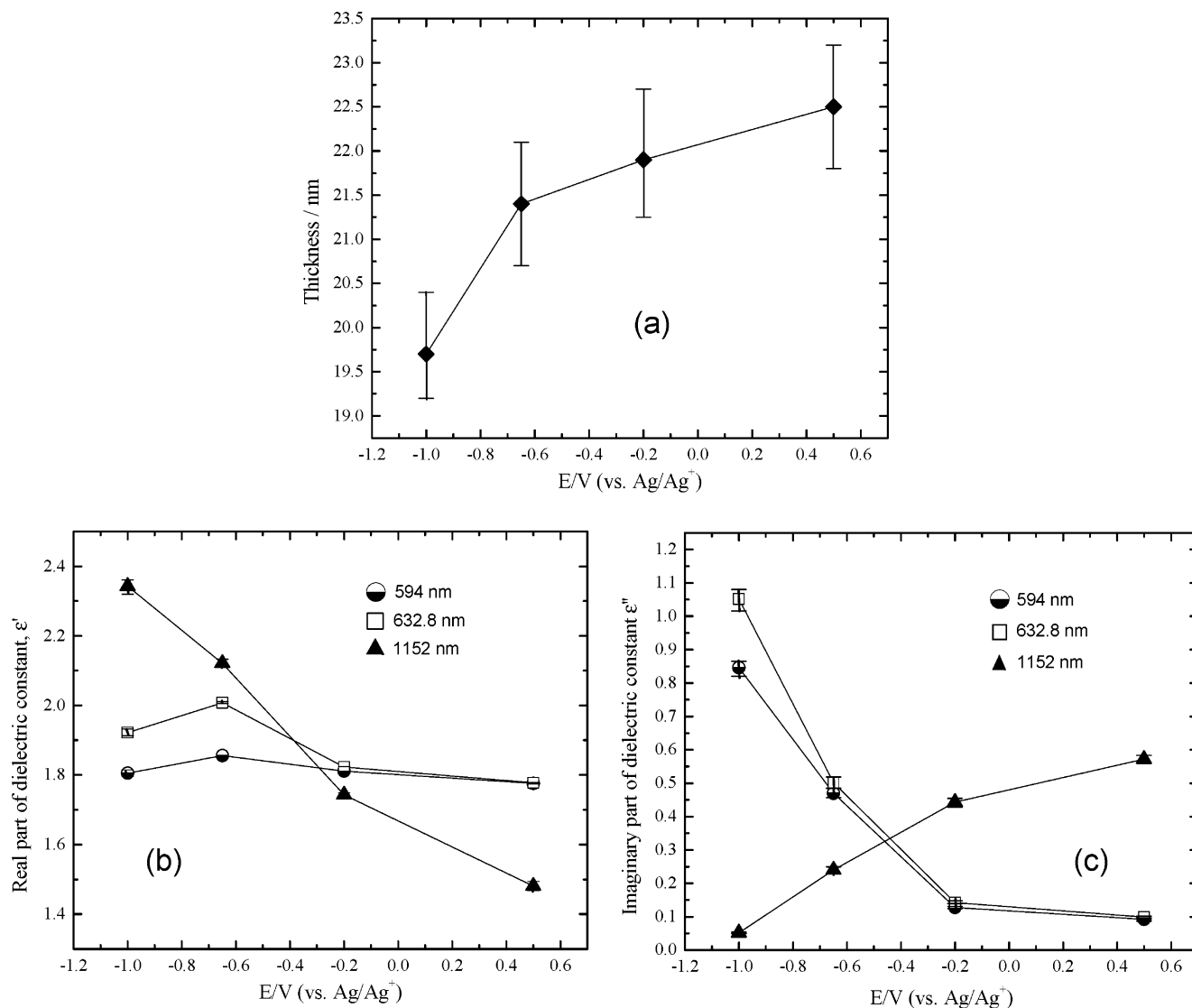


**Figure 7.** The thickness (a), real part  $\epsilon'$  (b), and imaginary part  $\epsilon''$  (c) of the dielectric constants as a function of the applied potential, measured at  $\lambda = 594$  nm,  $\lambda = 632.8$  nm, and  $\lambda = 1152$  nm.

experiments are taken at around this time after the corresponding potential was applied.

**Electrochemical SPR.** As shown in the UV-vis-NIR absorption spectra, the neutral polymer film has an absorption peak at around  $\lambda = 610$  nm. Upon oxidation, this absorption maximum decreases, and the absorption at longer wavelengths in the NIR region increases gradually. In particular, the absorption decreases at  $\lambda = 594$  nm and  $\lambda = 632.8$  nm and increases at  $\lambda = 1152$  nm upon doping.

The electrochromic behavior of an ultrathin PEDOT film was studied via the SPR response measured at three laser wavelengths ( $\lambda = 594$  nm,  $\lambda = 632.8$  nm, and  $\lambda = 1152$  nm). Figure 6 shows the SPR curves of a PEDOT film prepared at a constant potential ( $E = 0.9$  V). From the amount of charge applied, the thickness of this film at an open circuit potential was estimated to be about 22.5 nm using the correlation with the QCM data shown in Figure 2. The angular measurements at each potential ( $-1.0$ ,  $-0.65$ ,  $-0.2$ , and  $0.5$  V) were performed 2.5 min after changing the potential with all the other experimental conditions being the same as for the EQCM measurements in Figure 5. For each wavelength, the resonance angle and the shape of the SPR curves changed significantly in going from the doped state to the de-doped

state of the polymer film. For all wavelengths, the resonance peaks shifted to higher angles; however, at  $\lambda = 594$  nm and  $\lambda = 632.8$  nm, the curve became broader and the reflectivity values at the minimum of the resonance increased upon de-doping. Only for  $\lambda = 1152$  nm did the resonance dip become deeper and sharper upon de-doping.

Fitting of the experimental SPR reflectivity curves was done by Fresnel calculations using the thickness values obtained by the QCM 2.5 min after changing the potential. As demonstrated in Figure 6, all fitting curves show excellent agreement with the experimental results, with parameters summarized in Figure 7. Drastic changes, both in the real part and in the imaginary part of the dielectric constants, were determined at each wavelength. The error bars in Figure 7 are based on the density fluctuation of the polymer upon doping/de-doping, that is, 1.45–1.55. Based on these calculations, the accuracy for the determination of the complex dielectric constant is estimated to be better than  $\pm 0.04$  for the real part and  $\pm 0.08$  for the imaginary part of the dielectric constant; that is, EC-SPR measurements are able to determine the complex dielectric constants of the conducting polymer films in the doped/de-doped state rather independently of the uncertainty of the film density. The tendency of the dielectric constant

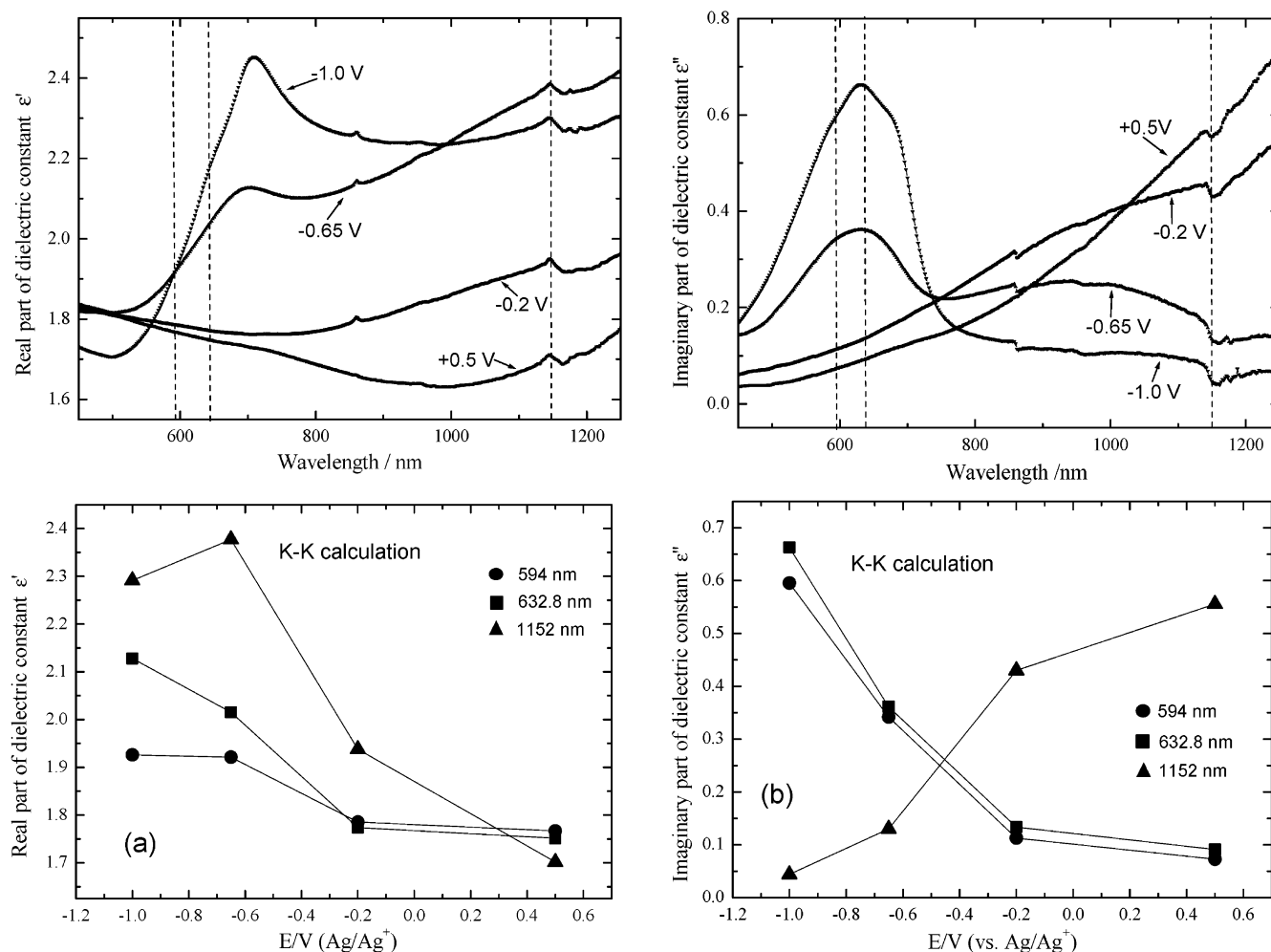


**Figure 8.** The complex dielectric constants obtained from the Kramers–Kronig calculation.

with wavelength is almost in good agreement with the result shown in Figure 8, which is obtained from the conventional optoelectrochemistry measurement (Figure 4) by using the Kramers–Kronig (K–K) relation as a function of wavelength and of potential. The different value in the imaginary part might be due to different conditions such as substrate (ITO) or film thickness (ca. 200 nm) in optoelectrochemistry measurements.

Thus, electrochromic phenomena of PEDOT films can be characterized by this EC-SPR technique with high sensitivity, which may lead to new designs for SPR-based sensors/biosensors based on the electrochromism of thin conducting polymer films.

**Optical Conductivity.** In EC-SPR experiments, it was found that the complex dielectric constants ( $\epsilon'$ ,  $\epsilon''$ ) varied strongly in going from the doped state (0.5 V) to the neutral state (−1.0 V). As the PEDOT film becomes conducting in the doped state, free carriers or intraband transitions cause the high value of the imaginary part of the dielectric constant at  $\lambda = 1152$  nm ( $E = 1.08$  eV), whereas few transitions from the valence band to the conduction band cause the low value of  $\epsilon''$  at  $\lambda = 594$  nm (2.09 eV) and  $\lambda = 632.8$  nm (1.96 eV), respectively. The employed energy ( $=1.08$  eV) is lower than that of the plasma frequency  $\omega_p$  ( $=1.2$  eV) reported for bulk PEDOT films.<sup>47</sup> However, the determined real part of the dielectric constant was positive in our experiments. This is equivalent to no evidence for a change in sign of the real part of the dielectric constant

even for energies as low as 0.001 eV and for the most metallic sample in the case of conducting polymers, and this observation is explained by the small fraction of delocalized carriers as reported by Lee et al.<sup>48</sup>

Since there is no anomalous dispersion at the intraband transition region ( $\lambda = 1152$  nm), we calculated the optical conductivity,  $\lambda = 1152$  nm, from the following equation.<sup>49</sup>

$$\epsilon(\omega) = \epsilon'(\omega) + i \frac{4\pi}{\omega} \sigma(\omega) \quad (2)$$

The calculated optical conductivity at  $\lambda = 1152$  nm is shown in Figure 9. Its value increases with potential, that is, with the level of doping, during which the electron is extracted from the valence band to the electrode by p-doping, and the polaron/bipolaron band is formed in the interband. The obtained  $\sigma$ -values at the doped state and the de-doped state are comparable to the ones reported from electrical conductivity measurements.<sup>1,50</sup> The accurate determination of electrical conductivities by the conventional techniques is very difficult, especially in situ, because the electrolyte in contact with the conducting

(48) Lee, K.; Miller, E. K.; Aleshin, A. N.; Menon, R.; Heeger, A. J.; Kim, J. H.; Yoon, C. O.; Lee, H. *Adv. Mater.* **1998**, *10*, 456.

(49) Georgiadis, R.; Peterlinz, K. A.; Rahn, J. R.; Peterson, A. W.; Grassi, J. H. *Langmuir* **2000**, *16*, 6759.

(50) Johansson, T.; Pettersson, L. A. A.; Inganäs, O. *Synth. Met.* **2002**, *129*, 269.

(47) Chang, Y.; Lee, K.; Kiebooms, R.; Aleshin, A.; Heeger, A. J. *Synth. Met.* **1999**, *105*, 203.

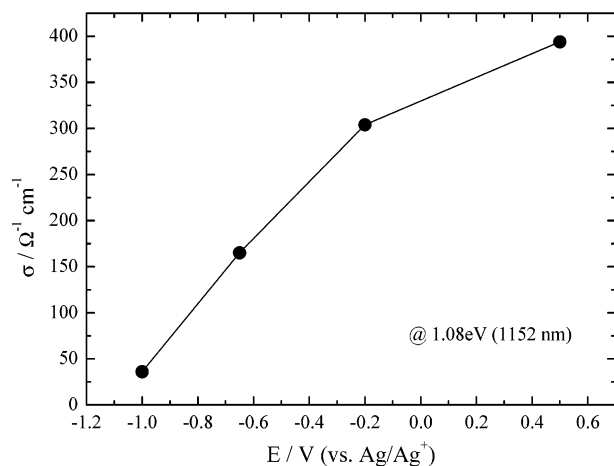


**Figure 9.** Optical conductivity measured at  $\lambda = 1152$  nm as a function of the applied potential obtained from EC-SPR data.

polymer film interferes with the measurement, with the doping levels of the ions changing with time even if the applied potentials are kept constant. Our results suggest that the optical determination of the conductivity of polymer films at different doping levels can be simply measured by the in situ EC-SPR technique using a NIR laser.

## Conclusions

The optical/electrochemical properties of poly(3,4-ethylenedioxythiophene) films were investigated by a combination of surface plasmon resonance spectroscopy and electrochemistry (EC-SPS). The dielectric constants at several doping levels were measured accurately with the film thickness being determined independently by the electrochemical quartz crystal microbalance. The EC-SPS measurements with three different wavelengths allow for the determination of the dielectric constants, both in the interband and in the intraband region of the electron transition. In particular, EC-SPS studies using a near-infrared laser allow for in situ measurements of the optical conductivity, resulting in values comparable to dc conductivity measurements.

**Acknowledgment.** This material is based upon work supported by the Science and Engineering Research Council under Grants R-152-000-037-303 (A\*STAR) and R-152-000-037-112 (MOE). We thank Dr. Kaloian Koykov (MPI-P) for helpful discussion on Kramers–Kronig calculations and Dr. Andreas Bund (Dresden University of Technology), Professor Rigoberto Advincula, and Dr. Ken Onishi (University of Houston) for helpful discussion. A.B. acknowledges the Max-Planck-Society for a postdoctoral fellowship.

LA034848N